Ars Pharmaceutica
https://revistaseug.ugr.es/index.php/ars
E-ISSN: 2340-9894 ISSN: 0004-2927

doi: 10.30827/ars.v66i4.33508
Artículos originales

Refining the Performance of Abiraterone Acetate through Industry-friendly Techniques for Improving Functionality

Refinando el rendimiento del acetato de abiraterona mediante técnicas industriales para mejorar la funcionalidad

Hardik Rana[1] 0000-0002-2159-7661
Vraj Khambholja[1] 0009-0004-8577-3981
Vaishali Thakkar[1] 0000-0001-6332-7703
Varsha Gadhvi [1] 0009-0000-9809-9851
Prachi Rabari[1] 0009-0002-9249-3983
Tejal Gandhi[1] 0000-0002-2011-1555

[1]Department of Pharmaceutics, Anand Pharmacy College, Anand, Gujarat, India.

Correspondence

Rana Hardik
hardikrana1439@gmail.com

Received: 11.04.2025
Accepted: 10.09.2025
Published: 20.09.2025

Acknowledgment

Authors would like to thank Anand Pharmacy College for providing infrastructure support to do experimental work.

Funding

Authors declare that they have no funding support for publication of this manuscript.

Conflict of interest

Authors declare no conflict of interest.

Abbreviations

Abiraterone Acetate (AA)
Gelucire 44/14 (GC44/14)
Neusilin (NS)
Fourier transform Infrared Spectroscopy (FTIR)
X-ray diffraction (XRD)
Differential scanning calorimetry (DSC)
Office of Generic Drugs (OGD)
Enzyme-free USP simulated intestinal fluid at pH 6.8 (SIF)
Quality by design (QbD)
Quality Target Product Profile (QTPP)
Critical quality attributes (CQAs)
Critical Process Parameters (CPPs)

Resumen

Introducción: El objetivo principal de este estudio fue mejorar la solubilidad y la permeabilidad del acetato de abiraterona mediante técnicas industrialmente viables.

Método: Se prepararon dispersiones sólidas de abiraterona con Gelucire 44/14, Dexolve y Eudragit EPO mediante diversas técnicas de mejora de la funcionalidad. Estas se caracterizaron por la solubilidad de fase, la disolución, la permeabilidad y las propiedades de flujo, mediante calorimetría diferencial de barrido, Espectroscopia Infrarroja por Transformada de Fourier y difracción de rayos X. Entre las técnicas y polímeros, se seleccionó el secado por aspersión con Gelucire debido a su mejora en la solubilidad. Se aplicó un diseño factorial completo de 32 para optimizar la dispersión sólida, centrándose en la disolución, la solubilidad y las propiedades de flujo (ángulo de reposo), siendo los atributos del material la relación abiraterona: Gelucire y la cantidad de neusilina. La región óptima se seleccionó a partir del gráfico de superposición.

Resultados: La dispersión sólida secada por aspersión mostró el mayor aumento de solubilidad con Gelucire en una proporción de 1:2, alcanzando un incremento de 405,94 veces. Los análisis mediante calorimetría diferencial de barrido, Espectroscopia Infrarroja por Transformada de Fourier y difracción de rayos X mostraron la transformación de la abiraterona de cristalino a amorfo. Los nueve lotes mostraron un %CDR que osciló entre el 30,85 % y el 90,33 % a los 30 minutos, con una solubilidad entre 141,049 µg/mL y 286,307 µg/mL. Las propiedades de flujo variaron de regulares a excelentes. El lote optimizado mostró una liberación del fármaco del 85,51 % a los 30 min, una solubilidad de 282,296 µg/mL y un buen flujo. Los estudios de permeabilidad ex vivo revelaron un 9,32 ± 0,147 % para la abiraterona y un 51,72 ± 0,286 %para el lote óptimo a los 90 min.

Conclusión: La solubilidad, la permeabilidad y la disolución aumentaron significativamente al preparar una dispersión sólida de abiraterona con Gelucire y neusilina mediante el método de secado por aspersión. Esta técnica sistemática y de fácil aplicación en la industria beneficiará al paciente.

Palabras clave: Abiraterona; mejora de la funcionalidad; Neusilina; secado por aspersión; Gelucire.

Abstract

Introduction: Main objective of this study was to enhance solubility and permeability of Abiraterone Acetate (AA) by industry-feasible techniques.

Method: Solid dispersion (SD) of Abiraterone with Gelucire 44/14 (GC44/14), Dexolve, and Eudragit EPO were prepared using various functionality-improving techniques. These properties were characterized by phase solubility, dissolution, permeability, flow properties, differential scanning calorimetry, Fourier transform Infrared Spectroscopy, and X-ray diffraction. Among various techniques and polymers, spray drying with Gelucire was selected based on its ability to enhance solubility. A 3^2 full factorial design was applied to optimize SD, focusing on dissolution, solubility, and flow property (angle of repose), with material attributes being Abiraterone: Gelucire ratio and Neusilin (NS) amount. Optimal region was selected from overlay plot.

Results: Spray-dried SD exhibited highest solubility, which increased with Gelucire at a 1:2 ratio, resulting in a 405.94-fold increase in solubility. DSC, FTIR, and XRD showed Abiraterone transformation from crystalline to amorphous. Nine batches showed a drug release ranging from 30.85% to 90.33 % at 30 minutes, with solubility between 141.049 µg/mL and 286.307 µg/mL. Angle of repose ranged from fair to excellent. Optimized batch exhibited 85.51% drug release at 30 min, a solubility of 282.296 µg/mL, and good flow. Ex vivo permeability studies revealed 9.32 ± 0.147 % for Abiraterone and 51.72 ± 0.286 % for optimal batch at 90 min.

Conclusion: Solubility, permeability, and dissolution increased significantly when a SD of Abiraterone was prepared with Abiraterone and Neusilin by spray drying method. Systematic, industry-friendly techniques will benefit patients.

Keywords: Abiraterone; functionality improvement; Neusilin; spray drying; Gelucire.

Highlights

- Use of an industry-friendly technique improved functionality of Abiraterone.
- Solid Dispersion was developed to comply with current regulatory guidelines.
- A combination of Gelucire and Neusilin was explored as a technique to improve flow ability of prepared Solid Dispersion.

Introduction

An unchecked proliferation of cells within prostate is indicative of prostate cancer[1]. Prostate cancer symptoms encompass challenges initiating urination, weakened or disrupted urine flow, discomfort or burning sensation during urination, and presence of blood in urine or semen, among others[2,3]. As per National Centre for National Informatics and Research, recorded cases of prostate cancer rose from 37,416 cases in 2016 to 41,532 in 2022 in India. It will exceed 47,000 cases in 2025. Prostate cancer is second most common type of cancer in men worldwide, accounting for 15% of cancer diagnoses in men[4]. Abiraterone Acetate (AA) is an innovative treatment for antiandrogen that aims to disrupt adrenal androgen-mediated signalling pathway[5]–[9]. AA is a Biopharmaceutical classification class IV drug, which has low solubility and poor permeability with bioavailability of only 10 %, resulting in low therapeutic outcomes. Due to all se issues and physicochemical properties, AA has become an area of interest for research to develop effective oral formulation[10,11]. A significant increase in effectiveness when taken with food[12]. Alternative methods to improve solubility and permeability of medicines with limited water solubility[13,14]. Creating SDs for poorly absorbable drugs effectively addresses drawbacks of se prior techniques[16, 17]. Current work aims to address issue of poor solubility and *in vitro* dissolution by reviewing various solubility enhancement techniques for SD. Goal of present study is also to review various types of carriers to select most suitable one for enhancing solubility.

Methodes

Materials

AA was received from Sun Pharmaceutical Industries Limited, India. Eudragit EPO was obtained from Evonik Industries, Germany. Gelucire 44/14 (GC44/14) and Dexolve were obtained from Cyclolab, Hungary. All other chemicals used were of analytical reagent grade.

Solubility estimation of AA

Solubility of AA was determined and expressed in mg/ml. solubility of AA was assessed using orbital shaker flask method in four media: Office of Generic Drugs (OGD) medium, enzyme-free USP simulated intestinal fluid pH 6.8, PBS pH 7.4, and distilled water[18]. An excess amount of AA was added to 10 mL flasks containing respective media, which were then sealed and incubated at 37°C with shaking at 120 rpm for 48 h. After incubation, 1 mL of supernatant was collected and analyzed using a UV-visible spectrophotometer (UV-1900, Shimadzu, Japan) to determine solubility.

Solubility enhancement technique

SD with different mass or molar mass ratios of AA and carrier was prepared using chosen techniques to identify best method for improving AA solubility. Following methods were used to prepare SDs.

Physical mixing

AA and carriers GC44/14, Eudragit EP0, and Dexolve were accurately weighed and transferred into a glass mortar-pestle, and triturated[17]. AA carriers were chosen in 1:1, 1:2, and 1:3 proportions. GC44/14 and Eudragit EP0 were taken in mass ratio, whereas Dexolve was taken in molar mass ratio.

Kneading method

AA and carrier were mixed in a glass vessel. A required quantity of ethanol was added gradually while AA and carriers were triturated or mixed using a pestle and mortar to form a slurry for 60 min, dried for 8 h at 60 ˚C screened through 100 mesh sieve[18].

Solvent evaporation technique

As shown in Table 1, AA and carrier in mass or molar mass were dissolved in a suitable quantity of ethanol. Ethanol was removed at 60 ˚C for 8 h and mass was scrapped from mould, pulverized, and sieved[19].

Melting method

As shown in Table 1, AA and carrier were heated in an oil bath to attain a molten state, followed by cooling and solidification while maintaining continuous stirring. Solid mass was then crushed, pulverized, and sieved to achieve desired particle size.

Spray drying

As shown in Table 1, AA and GC44/14 were dissolved in ethanol and transferred through a peristaltic pump into two inner lines of two-fluid nozzle with atomization air to obtain dried powder[22,23]. Inlet (80°C) and outlet temperature (40°C), Aspirator flow rate (65 Nm^3/hr), Feed Pump Flow Rate (5 ml/m) and oxygen percentage (5%) were set[22]–[24].

Solubility determination

Phase solubility was determined using technique described by Higuchi and Connor. An excess of SDs and AA was added distilled water and further followed same method as specified in solubility determination of AA[25,26].

Gibbs free energy

Gibbs's free energy was calculated for each dispersion. Negative Gibbs free energy values are associated with improved dissolution, confirming SD's ability to enhance drug's solubility in aqueous solutions. Solubility of drug (S_0) and solubility of SD (S_s) were calculated, and equation 1 was used to compute $\Delta G°_{tr}$ values of AA:

$$\Delta G^{\circ}_{tr} = 2.303RTLog\frac{S_0}{S_S}$$

Where S_o/S_s is ratio of molar solubility of AA before and after treatment. value of gas constant (R) is 8.31 J K^{-1} mol^{-1}, and T is temperature in degrees Kelvin[29].

Quality by design (QbD)

QbD is a proactive approach in drug formulation development that starts with predefined targets to ensure consistent product quality. Quality Target Product Profile (QTPP) which outlines ideal characteristics of drug product, ensuring its safety and efficacy. QTPPs serves as blueprint for designing product, from formulation to manufacturing[30]. Major target is to form SD of AA using spray dryer for adult to treat cancer through oral route. To meet se targets, identified critical quality attributes (CQAs) were solubility, dissolution and flow property. Identified Critical Process Parameters (CPPs) are amount of GC 44/14 and NS[29,30].

Experimental design

A 3^2 factorial design used to formulate nine experimental runs using Design Expert (V.13, Stat-Ease Inc., Minneapolis, USA). Design consists of two CMAs, GC: AA ratio (X_1), and amount of NS (X_2). Both CMAs X_1

(1:1, 1:2, 1:3) and X_2 (70, 95, 120) varied at three levels (-1, 0, and +1). %CDR at 30 minutes ($Y_1 \leq 80$ %), solubility ($Y_2 < 200$ µg/ml), and flow property ($Y_3 < 40^0$) were selected as CQAs. All nine batches were prepared and evaluated for chosen CQAs and or evaluation parameters.

Characterization of AA complex

Differential scanning calorimetry (DSC)

To evaluate physical changes that occurred in designed SD was evaluated by DSC using DSC-2 (STAR system, Mettler Toledo). Samples (2-4 mg) were heated in hermetically sealed, flat-bottomed aluminum pans under a nitrogen flow (20 mL/min) at a scanning rate of 10 °C/min between 25 °C and 200 °C. Empty aluminium pans served as reference standard[31].

Fourier transform infrared spectroscopy (FTIR)

SD was analyzed using a FTIR (Spectrum Two, PerkinElmer) to evaluate variation in functional groups compared to AA. Technique involved scattering a sample in KBr, mashed, and compacted into pellets. Pellets were placed in light path, and spectra were collected with a resolution of 2 cm^{-1} throughout a frequency range of 4000 to 400 cm^{-1} background spectrum of KBr was used as a blank for measurement[32,33].

Powder X-ray diffraction (XRD)

Sample was glued on a glass slide with vacuum grease, ensuring a uniform thickness of 0.5 mm. Slide was vertically positioned in X-ray diffractometer at 0°, with a Cu K-α 1 tube set to 40 KV and 50 mA as X-ray source. A scan from 2 to 600 2θ was performed at 0.0122 2θ/s, allowing for a comprehensive investigation of sample's crystal structure and arrangement[23,34].

Drug content of SD

Drug content or assay of SD was calculated by dissolving a SD equivalent to 50 mg of AA in 50 mL of Acetonitrile. solution was sonicated for 10 min and assayed at 254 nm for AA[39,40].

In-vitro dissolution study

Dissolution studies were conducted in OGD media at 37°C using a USP II paddle apparatus with a rotation speed of 50 rpm. 5 mL of dissolving medium was withdrawn at intervals and an equivalent fresh dissolving medium was replaced immediately. Test samples were filtered through a 0.45 µm Whatman filter, diluted as needed, measured for AA amount using a UV/VIS spectrophotometer at 255 nm.

Ex-vivo permeability study

Everted gut sac technique was employed to conduct a permeability study. Rat intestine was used, and fecal matter was flushed out of with Ringer solution. Intestine (2-4 cm) was inverted with assistance of a glass rod and blocked at one end with a thread. Ringer solution was infused into intestine and sealed at or end with assistance of thread. Sac was kept in a 250 mL Ringer solution with drug or SD glass beaker was used. Assembly was placed onto magnetic stirrer for 90 minutes. After 90 minutes, intestine was opened carefully from one side, and solution was drawn, filtered, diluted and measured for AA amount[41, 42].

Stability study

Optimized formulation was subjected to accelerated stability study. Experiment was conducted for six months at eir 40°C and 75% RH or 25°C and 60 % RH. After six month, sample was withdrawn and examined for physical and chemical observation[39,40].

Results

Solubility assessment

Solubility of AA is influenced by various factors, including physical and chemical properties of both solute and solvent[41]. Solubility of AA in different media was observed to be very low. Solubility in water (3.05±0.01 µg/mL), SIF (0.002±0.02 µg/mL), and OGD media (3.35±0.02 µg/mL).

Identification of industry-friendly technique

Phase solubility of SD was manufactured by varied techniques. SD prepared with GC44/14 with a 1:2 ratio has highest fold increment solubility amongst various methods (Table 1). favorable condition for AA solubilization was assessed by $\Delta G°_{tr}$ values[42]. Negative values of $\Delta G°_{tr}$ signify advantageous circumstances.

Table 1: Evaluation of SD.

Name of Technique	Polymer	Ratio of AA: carrier	Solubility (µg/ml)	fold of increment	Gibbs free energy (ΔG^0) (J/K. mol)
Physical mixing	GC44/14	1:1	54.77 ± 0.45	77.66	-11219.43
		1:2	112.03 ± 0.04	158.84	-13064.16
		1:3	70.54 ± 2.92	100.01	-11871.60
	Eudragit EPO	1:1	0.91 ± 0.09	1.29	-664.98
		1:2	1.04 ± 0.21	1.47	-994.51
		1:3	1.08 ± 0.043	1.53	-1095.61
	Dexolve	1:1	13.28 ± 4.09	18.83	-7566.50
		1:2	17.43 ± 3.08	24.71	-8267.49
		1:3	21.58 ± 0.42	30.59	-8818.04
Kneading	GC44/14	1:1	58.92 ± 0.62	83.54	-11407.67
		1:2	116.18 ± 0.99	164.73	-13157.91
		1:3	74.69 ± 4.52	105.90	-12018.95
	Eudragit EPO	1:1	1.00 ± 0.28	1.41	-889.28
		1:2	1.08 ± 0.55	1.53	-1095.61
		1:3	1.16 ± 0.89	1.65	-1286.65
	Dexolve	1:1	12.45 ± 1.23	17.65	-7400.13
		1:2	17.01 ± 3.42	24.12	-8205.37
		1:3	21.16 ± 0.13	30.00	-8767.99
Melting method	GC44/14	1:1	114.94 ± 0.66	162.96	-13130.14
		1:2	236.51 ± 0.09	335.34	-14990.34
		1:3	100.83 ± 0.23	142.96	-12792.56
	Eutragit EPO	1:1	1.70 ± 0.33	2.41	-2269.74
		1:2	1.78 ± 0.62	2.53	-2392.52
		1:3	1.95 ± 0.72	2.77	-2621.81
	Dexolve	1:1	Not performed due to high melting point of Dexolve.		
		1:2			
		1:3			

Name of Technique	Polymer	Ratio of AA: carrier	Solubility (µg/ml)	fold of increment	Gibbs free energy (ΔG^0) (J/K. mol)
Solvent Evaporation	GC44/14	1:1	156.43 ± 1.59	221.79	-13924.69
		1:2	278.01 ± 0.12	394.17	-15407.02
		1:3	142.32 ± 0.49	201.79	-13681.05
	Eudragit EPO	1:1	1.74 ± 4.05	2.47	-2331.86
		1:2	1.87 ± 3.42	2.65	-2509.71
		1:3	2.12 ± 2.42	3.00	-2832.36
	Dexolve	1:1	133.61 ± 0.09	189.44	-13518.19
		1:2	152.28 ± 2.63	215.91	-13855.39
		1:3	168.88 ± 1.25	239.44	-14122.07
Spray dryer	GC44/14	1:1	150.21 ± 0.82	212.97	-13820.03
		1:2	286.31 ± 5.23	405.94	-15482.84
		1:3	143.98 ± 0.09	204.14	-13710.94

Optimization of SD

A 3^2 FFD was employed to determine optimal set of CMAs, X_1 and X_2, to achieve required CQAs, Y_1, Y_2, and Y_3, as shown in Table 2. Quadratic model, based on a polynomial equation, is calculated using multiple correlation coefficient (R^2), adjusted multiple correlation coefficient (adjusted R^2), and predicted residual sum of squares of responses. Complete model was stripped of factors that were not significant ($P > 0.05$). Positive coefficients demonstrate a synergistic influence on responses, whilst negative coefficients demonstrate an antagonistic effect[43]. According to Table 2, nine factorial batches were produced, and results are displayed.

Response Y_1

Quadratic model demonstrated a satisfactory fit ($R^2 = 0.929$) and is statistically significant ($p = 0.0144$), revealing a strong correlation between CMAs and Y_1. A^2 is highly significant ($p = 0.0032$) among variables, implying that a higher polymer concentration results in a lower time for drug release[48]. Based on Eq. 2, A, B, AB, A^2, and B^2 have a positive impact on Y_1. Figure 1a indicate that an increase in polymer concentration enhances drug release up to a point —specifically, when polymer amount is double that of drug. Beyond this ratio, further increase in polymer content leads to retardation in drug release, indicating threshold effect.

$$Y_1 = 85.52 + 12.42\mathrm{A} - 0.4950\mathrm{B} - 1.55\mathrm{AB} - 32.17A^2 + 0.0683B^2$$

Response Y_2

Quadratic model for Y_2 response demonstrated a high correlation with CMAs ($R^2 = 0.9916$) and is statistically significant ($p < 0.0001$), indicating its reliability. A^2 had a significant effect ($p < 0.0001$), indicating that solubility increases when polymer concentration is doubled compared to drug concentration. Figures 1b indicated that drug-to-polymer ratio has a significant effect on Y_2. Solubility increases with increasing polymer concentration, reaching a maximum when polymer concentration is approximately twice that of drug. This increase is attributed to improved wettability of drug, lower crystallinity, and higher surface area in SD. Nevertheless, beyond this ideal proportion, increased levels of polymer content contribute to a decrease in solubility, likely due to elevated viscosity and decreased drug diffusion, which hinder effective dissolution.

$$Y_2 = 282.30 - 3.39\mathrm{A} - 0.5533\mathrm{B} - 0.2075\mathrm{AB} - 136.72A^2 + 2.90B^2$$

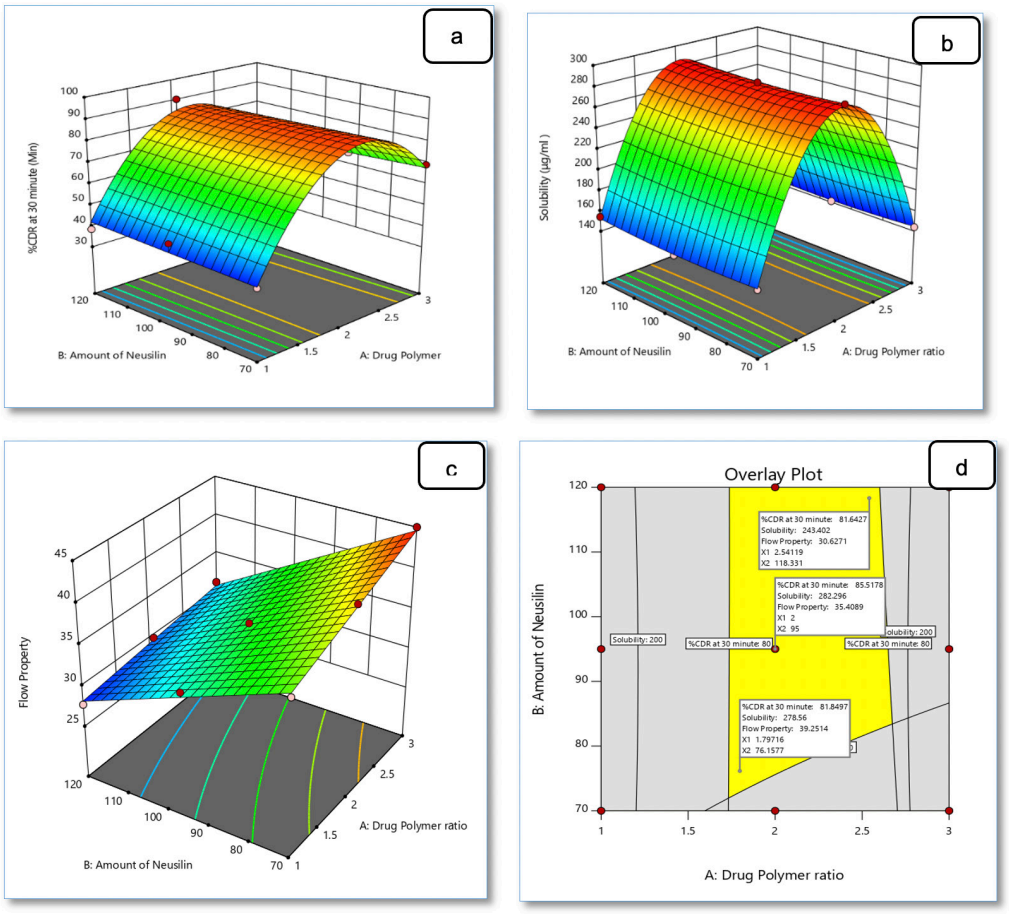

Figure 1: 2D and 3D plot for Y_1 (a), Y_2 (b), Y_3 (c), overlay plot (d).

Response Y_3

A 2FI model for Y_3 exhibited an excellent model fit ($R^2 = 0.9831$) and high statistical significance ($p < 0.0001$), indicating a strong correlation between CMAs and Y_3. A, B, and AB were significant ($p < 0.05$), highlighting ir combined effect on Y_3. Figure 1c reveals that higher polymer levels reduce flow due to ir waxy, cohesive texture, while NS enhances flow by improving powder fluidity and reducing inter-particle friction. It also suggest that optimizing both excipient levels is crucial for achieving desirable flow properties, which are essential for efficient processing, uniform mixing, and consistent dosage during SD formulation.

$$Y_3 = 35.41 + 2.29A - 5.91B - 0.9925AB$$

Table 2: Design Matrix.

Formulation number	X_1	X2 (mg)	Y1 (%)	Y2 (mg/mL)	Y3 (˚)
F1	1:1	95	45.02 ±0.02	148.13±0.05	33.69 ± 0.74
F2	1:1	120	38.5 ± 0.03	154.35±0.01	27.76 ± 0.11
F3	1:1	70	39.4 ± 0.23	150.20±0.23	37.57 ± 0.55
F4	1:2	95	90.33 ±0.08	282.15±0.455	29.74 ± 0.13
F5	1:2	120	81.05 ±0.09	284.23 ±0.32	35.54 ± 0.69
F6	1:2	70	85.31 ±0.21	286.30±0.22	41.63 ± 0.51
F7	1:3	95	62.11 ±0.15	147.30±0.15	31.22± 0.52
F8	1:3	120	68.20 ±0.25	143.98±0.56	45 ± 0.30
F9	1:3	70	66.15 ±0.1	141.07±0.88	38.22±0.15

Optimal region and validation of design

An optimal region (Figure 1d) was obtained by superimposing contour plots of all regions. Checkpoint batches were formulated, evaluated for responses, and % prediction error was measured. % relative value was obtained, ranging from 0.041% to 1.41%. High association observed amongst actual and forecast values tested reliability of prediction and verified model.

Characterization of AA and SD

DSC

DSC scan of pure drug showed a sharp endormic peak at 149.32^0 °C, which decreased to 42.25 °C after preparation of SD (Figure 2a). Absence of a peak indicated that AA was converted in amorphous form. This conversion assures dissolution enhancement of AA[45].

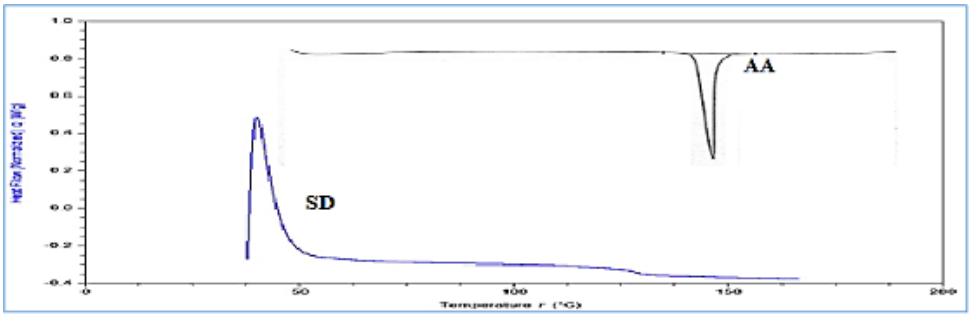

Figure 2: DSC thermogram (a) FTIR (b) and XRD (c).

FTIR

From Figure 3, it is evident that SD made with AA and GC44/14 exhibited IR peaks that retained well, indicating y were closely aligned with functional group of AA IR peaks, suggesting no interaction between drug and carrier.

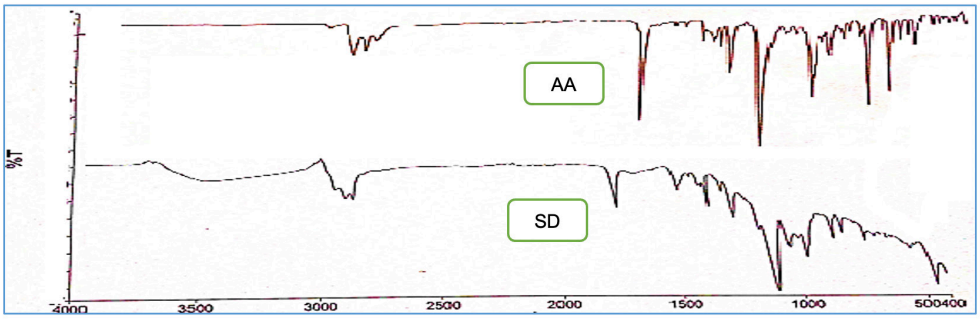

Figure 3: FTIR of AA and SD

XRD

XRD spectrum of pure AA and SD is shown in Figure 4. XRD spectra of AA show sharp peaks at diffraction angle (2ta) values of 18.45^0, 15.15^0, 21.79^0, 12.14^0, and 21.8^0. Number of peaks and peak height in diffractograms of SD were found to be decreased, exhibiting less intense peaks compared to AA, indicating a decrease in crystallinity. Results indicated an increase in solubility of AA.

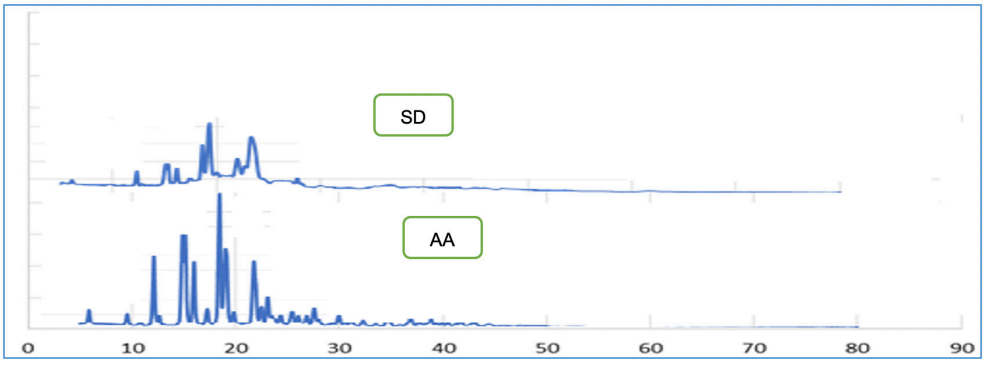

Figure 4: XRD of AA and SD

Evaluation of designed batches

Carr's index and Hausner's ratio were calculated from data on bulk density and tapped density. Angle of repose was also measured in triplicate. Results showed that flow property of designed SD was fair to excellent. NS had a significant positive effect on flowability. AA content of all DoE batches ranged from 97.68% to 99.68%, indicating that AA is uniformly distributed within SD.

From *vitro* release study, it was found that amount of GC44/14 has a significant effect on dissolution. It shows that when amount of GC44/14 increases, drug release also increases till a specific concentration of GC44/14. Complete AA release was observed in formulation within 45 min. whereas 40% AA release was observed with pure drug. A drastic improvement in %CDR was observed[18,51].

Permeability study was performed by everted gut sack method. In that only 9.32 ± 0.147 of pure drug sample permeates through intestinal membrane, whereas 51.72 ± 0.286 drug permeates from SD[47].

A stability study of optimized SD was carried out to determine physical and chemical properties of formulation. Formulated SD was observed to be stable after six months under accelerated conditions as re are no changes in physical properties as well as solubility and dissolution rate.

Discussion

AA is a hydrophobic drug with poor water solubility and dissolution rate. Due to its poor solubility and permeability, it exhibits limited absorption and consequently poor bioavailability[4]. re is an excellent challenge for pharmaceutical technologists to create an efficient drug delivery system[12,48]. SD is the most preferred approach to improve solubility[17].

Efforts were made to prepare SD of AA for treatment of prostate cancer. To improve solubility and permeability, various techniques, including physical mixing, kneading, solvent evaporation, melting method, and spray drying[54], were explored to formulate SDs. Three different polymers, including Eudragit EPO, SBE-β-CD, and GC44/14, were investigated. AA has minimal solubility in aqueous media. Preliminary studies were performed to select technique and polymer. Phase solubility was performed to evaluate batches that resulted in SD with a 1:2 ratio of GC44/14, prepared by spray drying, which showed highest fold of increment in solubility (405-fold).

QbD is emerging to enhance assurance of a safe and effective drug supply to consumers and also offers promise to improve manufacturing quality performance[55]. CPPs and/or CMAs were identified for immediate-release formulations[56]. Optimization of formulation was performed using a 3^2 factorial design. Two CMAs were AA: GC44/14 ratio and amount of NS whereas CQAs were %CDR at 30 min, solubility, and flow property. Responses were evaluated using ANOVA analysis, a 3D surface plot, and a contour plot[57, 58].

An overlay plot was generated for validation of design. Optimized batch with AA: GC44/14 ratio 1:2 and an amount of NS of 95mg demonstrates a desired drug release of 85.51% at 30 minutes, solubility of 282.296mg/mL, and good flow properties. In FTIR study, all AA functional group peaks were present, indicating no significant interaction with GC44/14. DSC study shows peak at 45.25^0 °C and no peak at AA melting point, which confirms preparation of SD. XRD shows a reduction in crystalline peaks[59]. Permeability studies of AA and an optimized batch SD were performed, which found 9.32% ± 0.147 and 51.72% ± 0.286 at 90 minutes, respectively[42]. Optimized SD was subjected to short-term stability testing, which revealed no significant changes in physical appearance or drug release, indicating stability of formulation during storage.

References

1. Sankarapillai J, Krishnan S, Ramamoorthy T, Sudarshan KL, Mathur P. Descriptive epidemiology of prostate cancer in India , 2012 – 2019 : Insights from the National Cancer Registry Programme. Indian J Urol. 2024;40:167–73. doi:10.4103/iju.iju.

2. Schafer EJ, Laversanne M, Sung H, Soerjomataram I. Recent Patterns and Trends in Global Prostate Cancer Incidence and Mortality : An Update. Eur Urol. 2024;87:302–13. doi:10.1016/j.eururo.2024.11.013.

3. Ferlay J, Rebecca ME, Mph LS. Global cancer statistics 2022: GLOBOCAN estimates of incidence and mortality worldwide for 36 cancers in 185 countries. CA Cancer J Clin. 2024;74:229–63. doi:10.3322/caac.21834.

4. Beg S, Malik AK, Ansari MJ, Malik AA, Ali AMA, Theyab A, et al. Systematic Development of Solid Lipid Nanoparticles of Abiraterone Acetate with Improved Oral Bioavailability and Anticancer Activity for Prostate Carcinoma Treatment. ACS Omega. 2022;7:16968–79. doi:10.1021/ACSOMEGA.1C07254.

5. Fiala O, Hosek P, Korunkova H, Hora M, Kolar J, Windrichova J, et al. Enzalutamide or Abiraterone Acetate With Prednisone in the Treatment of Metastatic Castration-resistant Prostate Cancer in Real-life Clinical Practice: A Long-term Single Institution Experience. Anticancer Res. 2023;43:463–71. doi:10.21873/anticanres.16183.

6. Yanagisawa T, Kimura T, Mori K, Suzuki H, Sano T, Otsuka T, et al. Abiraterone acetate versus nonsteroidal antiandrogen with androgen deprivation therapy for high-risk metastatic hormone-sensitive prostate cancer. Prostate. 2022;82:3–12. doi:10.1002/pros.24243.

7. Oyman A, Başak M, Özçelik M, Özyükseler DT, Işık S, Yıldırım ME. Efficacy of abiraterone acetate in castration-resistant metastatic prostate cancer: A real-world data analysis. Asia Pac J Clin Oncol. 2021;17:e201–7. doi:10.1111/ajco.13426.

8. Danielak D, Krejčí T, Beránek J. Increasing the efficacy of abiraterone - from pharmacokinetics, through therapeutic drug monitoring to overcoming food effects with innovative pharmaceutical products. Eur J Pharm Sci. 2022;176. doi:10.1016/j.ejps.2022.106254.

9. Malik JA, Ahmed S, Momin SS, Shaikh S, Alafnan A, Alanazi J, et al. Drug Repurposing: A New Hope in Drug Discovery for Prostate Cancer. ACS Omega. 2023;8:56–73. doi:10.1021/ACSOMEGA.2C05821.

10. Solymosi T, Tóth F, Orosz J, Basa-Dénes O, Angi R, Jordán T, et al. Solubility Measurements at 296 and 310 K and Physicochemical Characterization of Abiraterone and Abiraterone Acetate. J Chem Eng Data. 2018;63:4453–8. doi:10.1021/acs.jced.8b00566.

11. Katekar R, Sen S, Riyazuddin M, Husain A, Garg R, Verma S, et al. Augmented experimental design for bioavailability enhancement: a robust formulation of abiraterone acetate. J Liposome Res. 2023;33:65–76. doi:10.1080/08982104.2022.2069811.

12. Schultz HB, Meola TR, Thomas N, Prestidge CA. Oral formulation strategies to improve the bioavailability and mitigate the food effect of abiraterone acetate. Int J Pharm. 2020;577:119069. doi:10.1016/j.ijpharm.2020.119069.

13. Almeida HM. Development of a resveratrol solid dispersion with enhanced oral bioavailability by the lyophilization method. ICBAS. 2024.

14. Tran P, Pyo YC, Kim DH, Lee SE, Kim JK, Park JS. Overview of the manufacturing methods of solid dispersion technology for improving the solubility of poorly water-soluble drugs and application to anticancer drugs. Pharmaceutics. 2019;11:1–26. doi:10.3390/pharmaceutics11030132.

15. Ha ES, Choi DH, Baek IH, Park H, Kim MS. Enhanced oral bioavailability of resveratrol by using neutralized eudragit e solid dispersion prepared via spray drying. Antioxidants. 2021;10:1–12. doi:10.3390/antiox10010090.

16. Choudhari M, Damle S, Saha RN, Dubey SK, Singhvi G. Formulating abiraterone acetate-HPMCAS-based amorphous solid dispersions: insights into in vitro and biorelevant dissolution assessments and pharmacokinetic evaluations. RSC Adv. 2024;14:38492–505. doi:10.1039/d4ra08163c.

17. Malkawi R, Malkawi WI, Al-Mahmoud Y, Tawalbeh J. Current Trends on Solid Dispersions: Past, Present, and Future. Adv Pharmacol Pharm Sci. 2022;2022. doi:10.1155/2022/5916013.

18. Wagh VT, Gilhotra RM, Wagh RD. Solid dispersion (Kneading) technique: A platform for enhancement dissolution rate of valsartan poorly water soluble drug. Int J Pharm Qual Assur. 2020;11:20–4. doi:10.25258/ijpqa.11.1.3.

19. Asim M, Nazir M, Chauhdary Z, Irfan M, Khalid SH, Asghar S, et al. Enhanced Solubility and Biological Activity of Dexibuprofen-Loaded Silica-Based Ternary Solid Dispersions. Pharmaceutics. 2023;15. doi:10.3390/pharmaceutics15020399.

20. Hassan F, Sher M, Hussain MA, Saadia M, Naeem-Ul-Hassan M, Rehman MF ur, et al. Pharmaceutical and Pharmacological Evaluation of Amoxicillin after Solubility Enhancement Using the Spray Drying Technique. ACS Omega. 2022;7:48506–19. doi:10.1021/acsomega.2c06662.

21. Zhang J, Guo M, Luo M, Cai T. Advances in the development of amorphous solid dispersions: The role of polymeric carriers. Asian J Pharm Sci. 2023;18:100834. doi:10.1016/j.ajps.2023.100834.

22. Sharma U, Agrawal S, Chhajed M, Dwivedi S. Improved Dissolution and Solubility Characteristics of Clopidogrel Bisulphate using Gelucire 44/14. Eur J Parenter Pharm Sci. 2024;29. doi:10.37521/ejpps.29103.

23. Inam S, Irfan M, Lali NUA, Syed HK, Asghar S, Khan IU, et al. Development and Characterization of Eudragit® EPO-Based Solid Dispersion of Rosuvastatin Calcium to Foresee the Impact on Solubility, Dissolution and Antihyperlipidemic Activity. Pharmaceuticals. 2022;15. doi:10.3390/ph15040492.

24. Carvalho Feitosa R, Souza Ribeiro Costa J, van Vliet Lima M, Sawa Akioka Ishikawa E, Cogo Müller K, Bonin Okasaki F, et al. Supramolecular Arrangement of Doxycycline with Sulfobutylether-β-Cyclodextrin: Impact on Nanostructuration with Chitosan, Drug Degradation and Antimicrobial Potency. Pharmaceutics. 2023;15. doi:10.3390/pharmaceutics15041285.

25. Choi MJ, Woo MR, Choi HG, Jin SG. Effects of Polymers on the Drug Solubility and Dissolution Enhancement of Poorly Water-Soluble Rivaroxaban. Int J Mol Sci. 2022;23. doi:10.3390/ijms23169491.

26. Maulvi FA, Dalwadi SJ, Thakkar VT, Soni TG, Gohel MC, Gandhi TR. Improvement of dissolution rate of aceclofenac by solid dispersion technique. Powder Technol. 2011;207:47–54. doi:10.1016/j.powtec.2010.10.009.

27. Kanojiya PS, Charde Y, Avari JG, Wadetwa RN. Solid Dispersion of Lumefantrine Using Soluplus® by Solvent Evaporation Method: Formulation, Characterization and in-vitro Antimalarial Screening. Indian J Pharm Educ Res. 2022;56:121–32. doi:10.5530/ijper.56.1.15.

28. Buya AB, Mahlangu P, Witika BA. From lab to industrial development of lipid nanocarriers using quality by design approach. Int J Pharm X. 2024;8:100266. doi:10.1016/j.ijpx.2024.100266.

29. Gude R. Solubility enhancement and quality by design (qbd) assisted fabrication of fast dissolving buccal film for risperidone. IJPSR. 2023;14:459–81. doi:10.13040/IJPSR.0975-8232.14(1).459-81.

30. Wathore SA, Chhajed M, Singh M. To Design QBD (Quality-by-Design) Approach to Understand the Processing Factors Impact Melt-Extruded Solid Dispersions with an Instantaneous Release. Int J Pharm Biol Sci Arch. 2024;12:109–18.

31. Liu Y, Li Y, Xu P, Shen Y, Tang B, Wang Q. Development of Abiraterone Acetate Nanocrystal Tablets to Enhance Oral Bioavailability: Formulation Optimization, Characterization, In Vitro Dissolution and Pharmacokinetic Evaluation. Pharmaceutics. 2022;14. doi:10.3390/pharmaceutics14061134.

32. Shahoud S, Abdlwahed W, Hammad T. Development a taste-masked acetaminophen solid dispersions using Eudragit® E100 polymer by solvent evaporation technique. J Res Pharm. 2023;27:1998–2006. doi:10.29228/jrp.479.

33. Wang J, Huang B, Dai J, Chen G, Ren L. Inclusion complex of lurasidone hydrochloride with Sulfobutylether-β-cyclodextrin has enhanced oral bioavailability and no food effect. Am J Transl Res. 2022;14:1495–506.

34. Fan W, Zhang X, Zhu W, Zhang X, Di L. Preparation of curcumin-eudragit® EPO solid dispersions with gradient temperature through Hot-Melt extrusion. Molecules. 2021;26. doi:10.3390/molecules26164964.

35. Chi KN, Rathkopf D, Smith MR, Efstathiou E, Attard G, Olmos D, et al. Niraparib and Abiraterone Acetate for Metastatic Castration-Resistant Prostate Cancer. J Clin Oncol. 2023;41:3339–51. doi:10.1200/JCO.22.01649.

36. Fouad SA, Malaak FA, El-Nabarawi MA, Zeid KA, Ghoneim AM. Preparation of solid dispersion systems for enhanced dissolution of poorly water soluble diacerein: In-vitro evaluation, optimization and physiologically based pharmacokinetic modeling. PLoS One. 2021;16:1–26. doi:10.1371/journal.pone.0245482.

37. Sitovs A, Mohylyuk V. Ex vivo permeability study of poorly soluble drugs across gastrointestinal membranes: acceptor compartment media composition. Drug Discov Today. 2024;29:104214. doi:10.1016/j.drudis.2024.104214.

38. Shi Q, Carrillo JC, Penman MG, Manton J, Fioravanzo E, Powrie RH, et al. Assessment of the Intestinal Absorption of Higher Olefins by the Everted Gut Sac Model in Combination with in Silico New Approach Methodologies. Chem Res Toxicol. 2022;35:1383–92. doi:10.1021/acs.chemrestox.2c00089.

39. Hu B, Lv Z, Chen G, Lu J. Polymer selection for amorphous solid dispersion of a new drug candidate by investigation of drug polymer molecular interactions. Pharmazie. 2023;78:185–95. doi:10.1691/ph.2023.2061.

40. Bukkapatnam V, Mukthinuthalapati MA, Routhu KC. Study on Stress Degradation Behaviour of Abiraterone Acetate in Film Coated Tablets and Identification of Major Stress Degradation Product by Liquid Chromatography-Ultraviolet-Electrospray Ionization-Mass Spectrometry. Indian J Pharm Sci. 2022;84:300–10. doi:10.36468/pharmaceutical-sciences.923.

41. Gala U, Miller D, Williams RO. Improved dissolution and pharmacokinetics of abiraterone through kinetisol® enabled amorphous solid dispersions. Pharmaceutics. 2020;12. doi:10.3390/pharmaceutics12040357.

42. Liu C, Desai KG, Liu C. Enhancement of Dissolution Rate of Valdecoxib Using Solid Dispersions with Polyethylene Glycol 4000. Drug Dev Ind Pharm. 2005;31:1–10. doi:10.1081/ddc-200043918.

43. Talla S, Wadher K, Umekar M, Lohiya RT. Formulation, Optimization and Evaluation of Solid Dispersion of Deferasirox Using Factorial Design. J Drug Deliv Ther. 2024;14:23–31. doi:10.22270/jddt.v14i5.6526.

44. Bertoni S, Albertini B, Passerini N. Effect of polyoxylglycerides-based excipients (Gelucire®) on ketoprofen amorphous solubility and crystallization from the supersaturated state. Int J Pharm. 2025;669:125030. doi:10.1016/j.ijpharm.2024.125030.

45. Tamizhmathy M, Gupta U, Shettiwar A, Shiva G. Journal of Drug Delivery Science and Technology Formulation of inclusion complex of Abiraterone acetate with 2-Hydroxy propyl-Beta-Cyclodextrin : physiochemical characterization , molecular docking and bioavailability evaluation 2023;82:104321.

46. Bakhrushina E, Buraya L, Moiseev E, Shumkova M, Davydova M, Krasnyuk I. Optimizing Abiraterone Delivery through Intratumoral In Situ Implant: A Prospective Pharmaceutical Development Approach. Sci Pharm. 2023;2:37–45. doi:10.58920/sciphar02020037.

47. Braeckmans M, Augustijns P, Mols R, Servais C, Brouwers J. Investigating the Mechanisms behind the Positive Food Effect of Abiraterone Acetate: In Vitro and Rat In Situ Studies. Pharmaceutics. 2022;14. doi:10.3390/pharmaceutics14050952.

48. Møller A, Schultz HB, Meola TR. The Influence of Solidification on the in vitro Solubilisation of Blonanserin Loaded Supersaturated Lipid-Based Oral Formulations. Eur J Pharm Sci. 2021;157:105640. doi:10.1016/j.ejps.2020.105640.

49. Mondal S, Sirvi A, Jadhav K, Sangamwar AT. Supersaturating lipid-based solid dispersion of atazanavir provides enhanced solubilization and supersaturation in the digestive aqueous phase. Int J Pharm. 2023;638:1–10. doi:10.1016/j.ijpharm.2023.122919.

50. Rana H, Dholakia M, Gohel M, Omri A, Thakkar V, Gandhi T. Demonstration of Advanced Data Mining Tools for Optimization of Pellets Employing Modified Extrusion-pelletization Technique. Curr Drug Ther. 2020;16:154–69. doi:10.2174/1574885515999201217155123.

51. Rana HB, Gohel MC, Dholakia MS, Gandhi TR, Omri A, Thakkar VT. Development of Sustained Release Pellets of Galantamine HBr by Extrusion Spheronization Technique Incorporating Risk based QbD Approach. Res J Pharm Technol. 2018;11.

52. Rana H, Panchal M, Thakkar V, Gandhi T, Dholakia M. Investigating in-vitro functionality and in-vivo taste assessment of eco-friendly Tadalafil Pastilles. Heliyon. 2024;10:e29543. doi:10.1016/j.heliyon.2024.e29543.

53. Rana H, Patel D, Thakkar V, Gandhi T. Atovaquone smart lipid system: Design, statistical optimization, and in-vitro evaluation. Food Hydrocoll Heal. 2023;4:100144. doi:10.1016/j.fhfh.2023.100144.

54. Benmore CJ, Benmore SR, Edwards AD, Shrader CD, Bhat MH. A high energy x-ray diffraction study of amorphous Indomethacin . J Pharm Sci. 2022;111:818–24.